

CC-LOSS: CHANNEL CORRELATION LOSS FOR IMAGE CLASSIFICATION

Zeyu Song,¹ Dongliang Chang,¹ Zhanyu Ma,¹ Xiaoxu Li,² and Zheng-Hua Tan³

¹ Beijing University of Posts and Telecommunications
{szy2014, changdongliang, mazhanyu}@bupt.edu.cn

² Lanzhou University of Technology
xiaoxulilut@gmail.com

³ Aalborg University
zt@es.aau.dk

ABSTRACT

The loss function is a key component in deep learning models. A commonly used loss function for classification is the cross entropy loss, which is a simple yet effective application of information theory for classification problems. Based on this loss, many other loss functions have been proposed, *e.g.*, by adding intra-class and inter-class constraints to enhance the discriminative ability of the learned features. However, these loss functions fail to consider the connections between the feature distribution and the model structure. Aiming at addressing this problem, we propose a channel correlation loss (CC-Loss) that is able to constrain the specific relations between classes and channels as well as maintain the intra-class and the inter-class separability. CC-Loss uses a channel attention module to generate channel attention of features for each sample in the training stage. Next, an Euclidean distance matrix is calculated to make the channel attention vectors associated with the same class become identical and to increase the difference between different classes. Finally, we obtain a feature embedding with good intra-class compactness and inter-class separability. Experimental results show that two different backbone models trained with the proposed CC-Loss outperform the state-of-the-art loss functions on three image classification datasets.

Index Terms— Deep Learning, Image Classification, Loss Function, Channel Attention.

1. INTRODUCTION

Nowadays, deep learning has become the major methodology in solving computer vision problems. Deep convolutional neural network (CNN) [1, 2, 3, 4] is an important type of deep learning models and has shown outstanding performance on several tasks, including image classification [5, 6, 7, 8], object detection [9, 10], and object segmentation [10, 11]. Image classification, among others, is a basic vision ability of

humans. It is a popular deep learning task and has been researched for decades.

The loss function is a key component in deep CNN models for the purpose of parameter estimation and prior information constraint. For instance, a commonly used loss function, the cross entropy loss (CE-Loss) [12, 13], measures the distance between two probability distributions which adds information entropy as prior information to classification problem. Training with the CE-Loss improves the classification performance by increasing the predicted Softmax probability of the actual label. It guides the deep learning model to learn separate features for different classes. However, the CE-Loss has two main issues that limit the performance of a CNN model for classification. Firstly, the high level features extracted by CNNs with the CE-Loss are only separable with each other but not discriminative enough [14], which can easily lead to over-fitting of the model and thus weak generalization performance. Secondly, the parameters of the deep CNN model are trained jointly with all the classes, which makes the high level features extracted by CNNs to be confused with each other and increases the difficulty of optimization.

Many improvements on loss functions [14, 15, 16, 17, 18, 19, 20, 21] have been made to address the first problem, by introducing constraints to the feature space for discriminative feature embedding. The center loss [16] calculates and updates the class centers within each mini batch, which leads to intra-class compactness. The sphereface loss [15] introduces an angular margin to optimize the intra-class and inter-class relationship simultaneously, which yields features that are more discriminative. The cosface loss [17] adds a cosine angular margin according to the target logits to gain better performance against the sphereface loss. The arcface loss [18] further develops the angular margin to an additive angular margin, using summation rather than multiplication for efficient training. The inter-class angular loss (ICAL) [19] and the focal inter class angular loss (FICAL) [22] also consider the angular constraints among classes. By using the

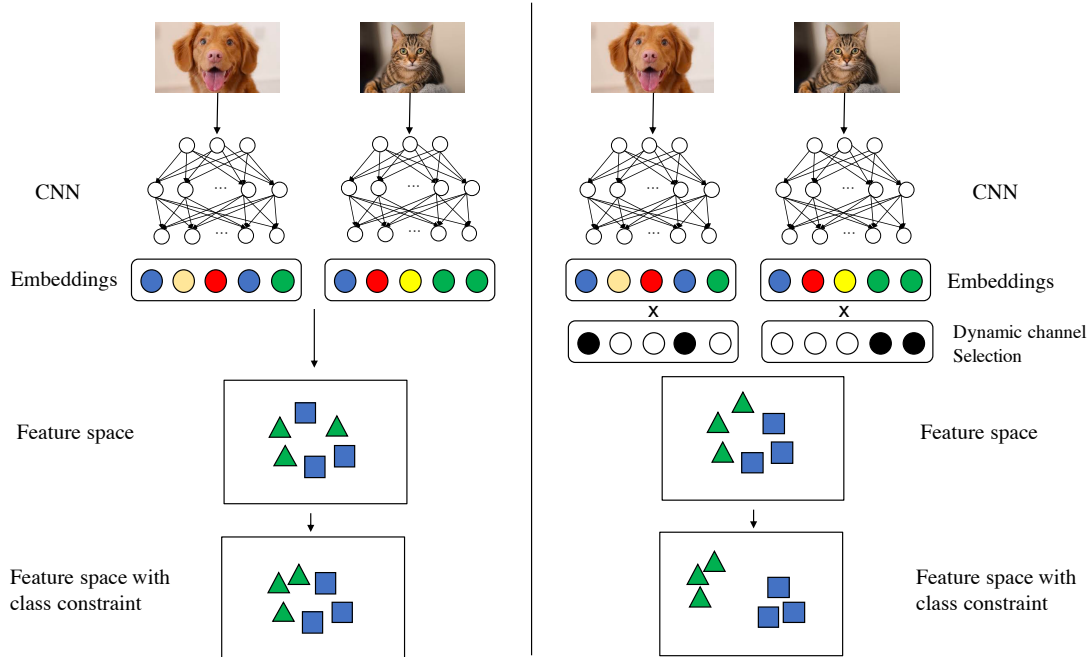


Fig. 1. Comparison between the CC-Loss and other related loss functions. The left column shows loss functions that only consider intra- and inter-class constraints. The right column shows the CC-Loss that enhances both the class relation constraints and feature discrimination.

cosine distances between the categories, these two loss functions both obtained higher classification accuracy among these loss functions. In addition to these improvements on loss functions for image classification, the focal loss [23] is a loss function proposed for object detection, assigning bigger weights to hard examples and smaller weights to easy examples to deal with class imbalance problem.

However, few loss functions have considered the second problem, *i.e.*, combining the network structure with intra-class and inter-class relationships to decrease the confusion between the features and reduce the difficulty of optimization. To handle this problem and motivated by the mutual channel loss [21], a recently proposed loss function that fixes the number of deep CNN channels for each class to obtain class-aligned features, we want to make different classes correspond to different channels of the features. This can make the samples belonging to different classes to train different parts of the deep CNN model and further learn the features from different classes to be distinguishable from each other. To this end, we propose a new loss function to align the channels to each sample. As shown in Fig. 1, for the samples from the same class, the proposed loss function can make the channel attention vectors be similar to each other. At the meantime, for the samples belong to different classes, the difference between the channel attention vectors will be increased. Finally, we can obtain high intra-class and low inter-class similarity features, which are beneficial for the image classification task.

The proposed loss function is termed as the channel correlation loss (CC-Loss). As shown in Fig. 2, it has two components that work together for feature embedding. Firstly, the squeeze-and-excitation module (SE module) [24] is introduced to generate channel attention for each sample, which is a widely used channel attention module in image classification. After that, we need to consider the intra-class and inter-class relations based on the channel attention vectors. Following the previous idea in the loss function design, a loss function needs to minimize the intra-class difference and maximize the inter-class difference. Therefore, the proposed CC-Loss calculates an Euclidean distance matrix of the attention vectors from one mini-batch. Each item of the calculated matrix represents the Euclidean distance between the channel attention vectors taken from two input images. By minimizing the sum of the Euclidean distances from the same class and maximizing the sum of the Euclidean distances from different classes simultaneously, the CC-Loss guided the CNN model to extract the features that have good intra-class compactness and inter-class separability.

The experiments have been conducted by applying the proposed CC-Loss on three commonly used datasets and two network architectures. Experimental results show that the models trained with the CC-Loss is able to extract more discriminative features and outperform the state-of-the-art methods.

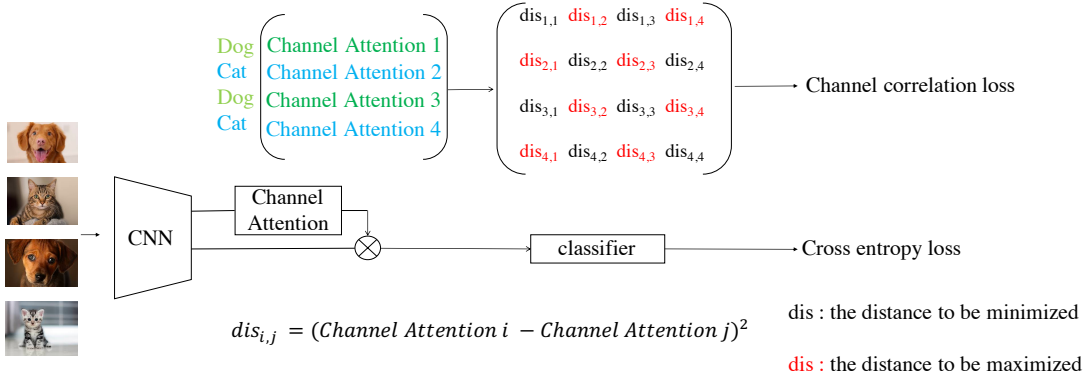


Fig. 2. The pipeline of the proposed CC-Loss. Channel attention vectors extracted from each sample are labeled with ground truth classes. The labeled channel attention vectors will then be used to calculate a distance matrix, representing the similarity between channel attentions of different samples. The similarity of samples belonging to the same class should be minimized while the similarity of samples belonging to the different class should be maximized. The distances between samples from the same class is marked in black and those from different classes are marked in red.

2. THE CC-LOSS FRAMEWORK

2.1. Channel attention module (CAM)

For the purpose of obtaining the channel attention vectors for each sample, we add the SE module to the classifier. The classifier in this work contains a hidden layer and a classification layer. The output of the hidden layer is the features, which are the input to the classification layer. We define the function of the hidden layer as $f_1(\cdot)$ and the function of the classification layer as $f_2(\cdot)$. Denote the features extracted from the CNN backbone as $F = \{F_1, F_2, \dots, F_N\}$, and the output of the classification layer is calculated as $P_1 = f_2(\text{ReLU}(f_1(F)))$.

Denote the function of the SE module as $f_{se}(\cdot)$ and the channel attention vector as $\mathbf{c} = \{c_1, c_2, \dots, c_n\}$ (n is channel numbers of features). The channel attention vector will be multiplied to the output vector of $f_1(\cdot)$ element-wise. Then the calculation process of the classifier will be $P_2 = f_2(\text{ReLU}(f_1(F) \cdot f_{se}(F)))$.

2.2. Channel Correlation Loss

The CE-Loss in each mini-batch can be defined as

$$L_{ce_1} = -\frac{1}{N} \sum_{n=1}^N \log\left(\frac{e^{P_1^{Y_n}}}{\sum_{i=1}^K e^{P_1^i}}\right), \quad (1)$$

where N is the batch size, K is the total number of classes, and Y_n is the label of the n^{th} sample.

In the CC-Loss, we use the channel attention vectors from one mini batch to represent the intra- and inter-class relationships. Hence, the channel attention matrix C is presented as

$$C = \begin{bmatrix} c_{1,1} & c_{1,2} & \cdots & c_{1,D} \\ c_{2,1} & c_{2,2} & \cdots & c_{2,D} \\ \vdots & \vdots & \ddots & \vdots \\ c_{N,1} & c_{N,2} & \cdots & c_{N,D} \end{bmatrix}_{N \times D}, \quad (2)$$

where $c_{i,j}$ is the j^{th} element in the channel attention vector of the i^{th} sample. N is the batch size and D is the dimensionality of the hidden layer.

Based on this design, we need to calculate the Euclidean distance between channel attention vectors to obtain the distance matrix from C . The distance between the channel attention vector of sample i and sample j is

$$d_{i,j} = \sum_{d=1}^D (c_{i,d} - c_{j,d})^2. \quad (3)$$

Now we obtain the distance matrix D of channel attention vectors for one mini-batch as

$$D = \begin{bmatrix} d_{1,1} & d_{1,2} & \cdots & d_{1,N} \\ d_{2,1} & d_{2,2} & \cdots & d_{2,N} \\ \vdots & \vdots & \ddots & \vdots \\ d_{N,1} & d_{N,2} & \cdots & d_{N,N} \end{bmatrix}_{N \times N}. \quad (4)$$

It is obvious that the Euclidean distance between the same sample will be $d_{i,i} = 0$ and the distance between the same sample pair is symmetric *i.e.*, $d_{i,j} = d_{j,i}$. Hence, we can further simplify the matrix to an upper triangular matrix as

$$D^{\text{UT}} = \begin{bmatrix} 0 & d_{1,2} & \cdots & d_{1,N} \\ 0 & 0 & \cdots & d_{2,N} \\ \vdots & \vdots & \ddots & \vdots \\ 0 & 0 & \cdots & 0 \end{bmatrix}_{N \times N}. \quad (5)$$

Now the distance matrix is simple enough to calculate the intra-class component and the inter-class component for the CC-Loss. The intra-class component is the sum of the distances within the same class. For example, if sample i and sample j are from the same class, $d_{i,j}$ is added to the intra-

class component. Hence, L_{intra} is calculated as

$$L_{intra} = \sum_{i=1}^N \sum_{j=i}^N d_{i,j} \cdot \mathbf{I}(Y_i, Y_j), \quad (6)$$

where the operator $\mathbf{I}(Y_i, Y_j)$ is defined as

$$\mathbf{I}(Y_i, Y_j) = \begin{cases} 1, & Y_i = Y_j \\ 0, & \text{otherwise} \end{cases}.$$

The inter-class component is the sum of distances from different classes. Therefore, L_{inter} is

$$L_{inter} = \sum_{i=1}^N \sum_{j=i}^N d_{i,j} \cdot [1 - \mathbf{I}(Y_i, Y_j)]. \quad (7)$$

The distances between the same class should be minimized, which forces the channel selection to be the same and enhances the intra-class compactness. Meanwhile, the distances among different classes should be maximized, which forces the channel selection to be different and enlarges the inter-class separability. Hence, the final loss function is defined as

$$L = L_{ce2} + \lambda \cdot \frac{L_{intra}}{L_{inter} + \epsilon}, \quad (8)$$

$$L_{ce2} = -\frac{1}{N} \sum_{n=1}^N \log\left(\frac{e^{P_2^{Y_n}}}{\sum_{i=1}^K e^{P_2^i}}\right), \quad (9)$$

where ϵ is a small positive constant and λ is a hyper-parameter.

2.3. Computational Complexity Reduction

The computational complexity to compute the distance matrix D is $O(N^2)$, while it is $O(N^2)$ for calculating L_{intra} and L_{inter} . Therefore, the overall computational complexity for CC-Loss is $O(N^2)$. In order to facilitate the calculation, we reduce the computational complexity of calculating the distance matrix from $O(N^2)$ to $O(N)$ by the following steps.

Each item $d_{i,j}$ in the distance matrix D is calculated as,

$$\begin{aligned} d_{i,j} &= \sum_{k=1}^D (c_{i,k} - c_{j,k})^2 \\ &= \sum_{k=1}^D c_{i,k}^2 + \sum_{k=1}^D c_{j,k}^2 - 2 \sum_{k=1}^D c_{i,k} c_{j,k}. \end{aligned} \quad (10)$$

Denote s_i as the square sum of each item of the i^{th} channel attention vector in C , which is given as,

$$s_i = \sum_{k=1}^D c_{i,k}^2, \quad (11)$$

we and then calculate two auxiliary matrix E and E^T with computational complexity $O(n)$. Here, matrix E is defined as,

$$E = \begin{bmatrix} s_1 & s_1 & \cdots & s_1 \\ s_2 & s_2 & \cdots & s_2 \\ \vdots & \vdots & \ddots & \vdots \\ s_N & s_N & \cdots & s_N \end{bmatrix}_{N \times N}. \quad (12)$$

After that, we calculate an auxiliary matrix $G = C \times C^T$ with $O(n)$, which is

$$G = \begin{bmatrix} c_{1,1} & c_{1,2} & \cdots & c_{1,D} \\ c_{2,1} & c_{2,2} & \cdots & c_{2,D} \\ \vdots & \vdots & \ddots & \vdots \\ c_{N,1} & c_{N,2} & \cdots & c_{N,D} \end{bmatrix} \times \begin{bmatrix} c_{1,1} & c_{2,1} & \cdots & c_{N,1} \\ c_{1,2} & c_{2,2} & \cdots & c_{N,2} \\ \vdots & \vdots & \ddots & \vdots \\ c_{1,D} & c_{2,D} & \cdots & c_{N,D} \end{bmatrix}. \quad (13)$$

Note that G is a $N \times N$ matrix and the item $g_{i,j}$ in G is

$$g_{i,j} = \sum_{k=1}^D c_{i,k} c_{j,k}. \quad (14)$$

Then, the matrix D is now calculated as $D = E + E^T - 2G$. The overall computational complexity is reduced to $O(N)$.

3. EXPERIMENTAL RESULTS AND DISCUSSIONS

In this section, the proposed CC-Loss is evaluated on three datasets: MNIST [25], CIFAR-100 [26], and Cars-196 [27]. Two CNN backbones, VGG16 and ResNet18, are investigated. Furthermore, we compare the CC-Loss with other loss functions including the CE-Loss [12], the Focal loss [23], the A-softmax loss [15], the inter-class angular loss (ICAL) [19], and the focal inter class angular loss (FICAL) [22].

3.1. Datasets description

MNIST [25] is a handwritten digits classification dataset contains numbers from zero to nine. It includes a training set with 60,000 images and a test set with 10,000 images. All the images have been normalized and resized to the size of 28×28 .

CIFAR-100 [26] is a natural scene image classification dataset that contains 60,000 colored images from 100 classes. The training set and the test set contain 50,000 and 10,000 images, respectively. All the images are with the resolution of 32×32 .

Cars-196 [27] is a fine-grained vehicle classification dataset, which contains 8,144 training images and 8,041 test images from 196 classes.

3.2. Implementation details

We applied the CC-loss function to two widely used CNN architectures, *i.e.*, VGG16 and ResNet18.

Table 1. Classification accuracy(%) with different loss functions. The backbone models were VGG16 and ResNet18 and evaluated on three datasets. All the CC-loss results are the average of five rounds evaluations.

Loss Function	Backbone Model	MNIST	CIFAR-100	Cars-196
CE Loss	VGG16/ResNet18	97.43/97.52	74.49/77.38	88.02/85.77
Focal Loss	VGG16/ResNet18	97.64/97.68	74.46/77.63	88.21/85.98
A-softmax Loss	VGG16/ResNet18	98.10/98.32	74.55/77.78	90.02/87.22
MC Loss	VGG16/ResNet18	98.20/98.45	72.51/70.18	92.80/-
ICAL	VGG16/ResNet18	97.83/98.21	74.79/77.71	89.32/86.67
FICAL	VGG16/ResNet18	98.22/98.40	74.98/78.18	89.70/87.38
CC-Loss	VGG16 + CAM/ResNet18 + CAM	98.32 ± 0.08/98.52 ± 0.09	75.49 ± 0.15/78.23 ± 0.07	91.46 ± 0.09/88.41 ± 0.06

Table 2. Ablation Study on the batch size for the CC-Loss. The experiments were conducted on CIFAR-100 as well as Cars-196 datasets with VGG16 backbone.

Batch Size	CIFAR-100	Cars-196
8	74.9 ± 0.12	91.3 ± 0.12
16	75.3 ± 0.07	91.5 ± 0.09
32	75.5 ± 0.15	91.3 ± 0.16
64	75.1 ± 0.14	90.6 ± 0.18
128	74.5 ± 0.14	89.9 ± 0.15

Table 3. The p values of one sample t -test.

Base Model	MNIST	CIFAR-100	Cars-196
VGG16	3.9×10^{-3}	4.7×10^{-4}	2.1×10^{-7}
ResNet18	3.3×10^{-3}	3.8×10^{-3}	4.3×10^{-7}

All the methods were trained with the stochastic gradient descent (SGD) [28] algorithm with 300 epochs. The batch sizes for MNIST, CIFAR-100, and Cars-196 were set to 32, 32, and 16, respectively. The input image sizes were 24×24 , randomly cropped 32×32 , and randomly cropped 224×224 following a zero padding with size 4 for MNIST, CIFAR-100, and Cars-196, respectively. Horizontally flipping with 0.5 probability was also applied when training CIFAR-100 and Cars-196. The initial learning rate was set to 0.1 and adjusted by the cosine annealing schedule [29] to $1e - 5$. We set the weight decay as $5e - 4$ and the momentum as 0.9. When training MNIST and CIFAR-100, the network parameters were initialized with the method in [30]. While training Cars-196, we used the ImageNet pretrained parameters as the initial ones. For the hyper-parameters of the loss functions used for comparison, we followed the referred papers. For the CC-Loss, we set λ to 1. All the experiments results reported shared the same hyper-parameters.

We conducted each of our experiments five rounds and report the average accuracy and margin in the form of *accuracy ± margin*. The margin is defined as maximum absolute difference between the five results and it’s average. For baseline methods in Table 1 and Table 4, we refer to results from [21] and [22], which only report average values.

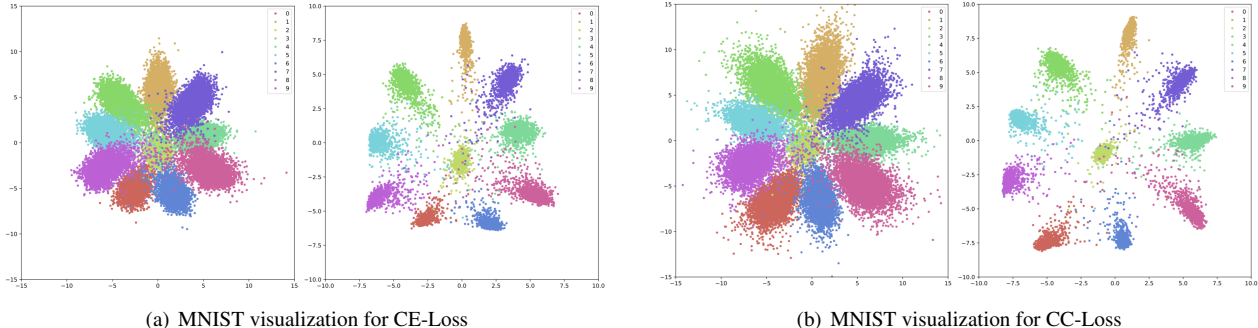
3.3. Comparison with state-of-the-art methods

As shown in Table 1, the proposed CC-Loss outperforms the CE-Loss by a large margin. For ResNet18, the CC-Loss improves the performance from 97.52% to 98.52%, 77.38% to 78.23%, and 85.77% to 88.41% on MNIST, CIFAR-100, and Cars-196 dataset, respectively. For VGG16, the CC-Loss outperforms the CE-Loss by 0.89%, 1%, and 3.33% on MNIST, CIFAR-100, and Cars-196, respectively. These results indicate the class relation constraints in the CC-Loss indeed help the CNN model with more discriminative features, which shows the effectiveness of the CC-Loss. The improvement on Cars-196 dataset is the most significant as the class relationship in the fine-grained image classification dataset is more complex. Therefore, it benefits more from the class relation constrains. The VGG16 backbone gets more improvement over ResNet18 for higher parameter numbers bring to higher model capacity, which react better with more prior information generated by CC-Loss. While comparing with the state-of-the-art loss functions that only focus on intra- and inter-class relations, the CC-Loss also shows competitive performance on all the three datasets. For ResNet18, CC-Loss gets slightly better results on MNIST and CIFAR-100 compared to the second best FICAL loss, and get 1.03% boosting performance on the Cars-196 dataset. For VGG-16, the CC-Loss gets 0.1% and 0.51% improvement against the FICAL loss on MNIST and CIFAR-100. It also gets 1.44% accuracy improvement compared with the second best A-softmax Loss. These demonstrate that the additional dynamic class-channel mechanism can help with the classification task.

Specifically, we further analyze the results of the MC-Loss, another loss function which focuses on channel-wise intra-class and inter-class relationship designed for the fine-grained visual classification (FGVC) task. The MC-Loss has better performance on the Cars-196 dataset, which is a FGVC dataset. But it has worse performance on image classification datasets, *i.e.*, MNIST and CIFAR-100. The key reason is that MC-Loss allocates constant channel numbers for each class (3 channels for each class in Cars-196) and learns three different feature maps for each class. While in general image classification tasks, there might not be enough separate feature map for each sample, this will yield sub-optimization of the feature maps and can not meet the separation constraint. Furthermore, using constant channel number is unsuitable for

Table 4. Ablation study of the channel attention module.

Loss Function	Backbone Model	MNIST	CIFAR-100	Cars-196
CE Loss	VGG16/ResNet18	97.43/97.52	74.49/77.38	88.02/85.77
CE Loss	VGG16 + CAM/ResNet18 + CAM	97.66 ± 0.02/97.67 ± 0.01	74.54 ± 0.02/77.57 ± 0.01	88.15 ± 0.03/86.04 ± 0.02
CC Loss	VGG16 + CAM/ResNet18 + CAM	98.32 ± 0.08/98.52 ± 0.09	75.49 ± 0.15/78.23 ± 0.07	91.46 ± 0.09/88.41 ± 0.06

**Fig. 3.** Visualization on MNIST dataset trained by CE-Loss and CC-Loss. The left sub-figure and the right sub-figure shows the results on training set and test set respectively.**Table 5.** The effect of λ in CC-Loss. The experiments were conducted using VGG16 + CAM as the backbone

λ	MNIST	CIFAR-100	Cars-196
0	97.66 ± 0.02	74.54 ± 0.02	88.15 ± 0.03
0.5	98.04 ± 0.05	75.12 ± 0.03	89.53 ± 0.07
1.0	98.32 ± 0.08	75.49 ± 0.15	91.46 ± 0.09
1.5	97.95 ± 0.06	75.04 ± 0.09	89.42 ± 0.05
2.0	97.53 ± 0.03	74.32 ± 0.12	87.84 ± 0.02

CIFAR and MNIST classes, which also causes a worse result of MC-Loss.

3.4. The effect of CAM

We add a channel attention model on top of the CNN backbone to meet the requirement of dynamic channel selection. An ablation study is proposed to show the performance of the channel attention module when CC-Loss is not applied. As shown in Table 4, in the case of w/o CC-Loss, dynamic channel selection gives slight improvement against the original backbone. When CC-Loss is used, it provides extra class relation constraint to boost the performance. Also, it is worth to note that CC-Loss can not be implemented without the CAM module.

3.5. The effect of weight in CC-Loss

As shown in Table 5, we evaluated the performance of different λ , representing the influence of CC-Loss. The best result is obtained when λ is 1. Further increasing λ will cause performance drop because we need class-label relationship pro-

vided by the CE-Loss.

3.6. Hyper-parameter tuning on batch size

Since we optimize the channel attention distances within mini-batches, the batch size is an important hyper-parameter to be tuned. We analyzed the affect of batch size on CIFAR-100 and Cars-196 datasets with VGG16 as the backbone. As shown in Table 2, a smaller batch size leads to a higher classification accuracy, since the class relationship in the distance matrix is simpler and easier to optimize. However, when the batch size tends to be very small, the class relationship will disappear and thus the accuracy is decreased. Therefore, we empirically chose a batch size of 32 for the CIFAR-100 dataset and a batch size of 16 for the Cars-196 dataset.

3.7. Statistical significance analysis

As the number of experiments is less than 30, we used the one sample unpaired t -test [31] to evaluate the statistical significance of the results. We took the values from the state-of-the-art method as the general average value for test. More specifically, we used the results from the A-softmax Loss for Cars-196 dataset on VGG16 backbone and the results from the FICAL Loss for the rest. As shown in Table 3, all the p -values of the one sample t -test with SOTA results are below 5×10^{-3} , which indicates statistically significant improvements obtained by the CC-Loss compared with the baseline loss functions.

3.8. Visualization

We carry out the visualization experiments by training VGG16 on the MNIST dataset. The output dimensionality of the first linear layer in VGG16 was set to 2. The features extracted

from the first linear layer are visualized to present the feature space obtained by the CE-Loss and the CC-Loss. From Fig. 3, it can be observed that the features from the CC-Loss are more compact within the same class while more separable among the neighbour classes. This demonstrates the effectiveness of intra-class and inter-class component of CC-Loss.

4. CONCLUSIONS

In this paper, we proposed a new loss function, namely the Channel Correlation Loss (CC-Loss), for the task of image classification. The CC-Loss dynamically selects the CNN channels for each class via the channel attention mechanism. It assigns larger numbers of channels to the harder classes and smaller numbers of channels to the easier class. Furthermore, by considering the Euclidean distances of the channel attention vectors in mini-batches, the CC-Loss is able to maximize both the intra-class compactness and the inter-class separability, which can extract more discriminative features. Experimental results on three datasets with two different backbones demonstrated that the proposed method outperforms commonly used loss functions.

5. REFERENCES

- [1] Alex Krizhevsky, Ilya Sutskever, and Geoffrey E Hinton, "ImageNet classification with deep convolutional neural networks," in *NeurIPS*, 2012.
- [2] Karen Simonyan and Andrew Zisserman, "Very deep convolutional networks for large-scale image recognition," *arXiv preprint arXiv:1409.1556*, 2014.
- [3] Gao Huang, Zhuang Liu, Laurens Van Der Maaten, and Kilian Q Weinberger, "Densely connected convolutional networks," in *CVPR*, 2017.
- [4] Kaiming He, Xiangyu Zhang, Shaoqing Ren, and Jian Sun, "Deep residual learning for image recognition," in *CVPR*, 2016.
- [5] Jia Deng, Wei Dong, Richard Socher, Li-Jia Li, Kai Li, and Li Fei-Fei, "ImageNet: A large-scale hierarchical image database," in *CVPR*, 2009.
- [6] Ruoyi Du, Dongliang Chang, Ayan Kumar Bhunia, Jiyang Xie, Yi-Zhe Song, Zhanyu Ma, and Jun Guo, "Fine-grained visual classification via progressive multi-granularity training of jigsaw patches," *arXiv preprint arXiv:2003.03836*, 2020.
- [7] Yixiao Zheng, Dongliang Chang, Jiyang Xie, and Zhanyu Ma, "Iu-module: Intersection and union module for fine-grained visual classification," in *2020 IEEE International Conference on Multimedia and Expo (ICME)*. IEEE, 2020, pp. 1–6.
- [8] Zhanyu Ma, Dongliang Chang, Jiyang Xie, Yifeng Ding, Shaoguo Wen, Xiaoxu Li, Zhongwei Si, and Jun Guo, "Fine-grained vehicle classification with channel max pooling modified CNNs," *IEEE Transactions on Vehicular Technology*, vol. 68, no. 4, pp. 3224–3233, 2019.
- [9] Tsung-Yi Lin, Michael Maire, Serge Belongie, James Hays, Pietro Perona, Deva Ramanan, Piotr Dollár, and C Lawrence Zitnick, "Microsoft COCO: Common objects in context," in *ECCV*, 2014.
- [10] Alina Kuznetsova, Hassan Rom, Neil Alldrin, Jasper Uijlings, Ivan Krasin, Jordi Pont-Tuset, Shahab Kamali, Stefan Popov, Matteo Mallocci, Tom Duerig, et al., "The open images dataset v4: Unified image classification, object detection, and visual relationship detection at scale," *arXiv preprint arXiv:1811.00982*, 2018.
- [11] Bolei Zhou, Hang Zhao, Xavier Puig, Sanja Fidler, Adela Barriuso, and Antonio Torralba, "Scene parsing through ADE-20k dataset," in *CVPR*, 2017.
- [12] Yi Sun, Xiaogang Wang, and Xiaoou Tang, "Deep learning face representation from predicting 10,000 classes," in *CVPR*, 2014.
- [13] Yaniv Taigman, Ming Yang, Marc Aurelio Ranzato, and Lior Wolf, "DeepFace: Closing the gap to human-level performance in face verification," in *CVPR*, 2014.
- [14] Binghui Chen, Weihong Deng, and Haifeng Shen, "Virtual class enhanced discriminative embedding learning," in *NeurIPS*, 2018.
- [15] Weiyang Liu, Yandong Wen, Zhiding Yu, Ming Li, Bhiksha Raj, and Le Song, "Sphereface: Deep hypersphere embedding for face recognition," in *CVPR*, 2017.
- [16] Yandong Wen, Kaipeng Zhang, Zhifeng Li, and Yu Qiao, "A discriminative feature learning approach for deep face recognition," in *ECCV*, 2016.
- [17] Hao Wang, Yitong Wang, Zheng Zhou, Xing Ji, Dihong Gong, Jingchao Zhou, Zhifeng Li, and Wei Liu, "Cosface: Large margin cosine loss for deep face recognition," in *CVPR*, 2018.
- [18] Jiankang Deng, Jia Guo, Niannan Xue, and Stefanos Zafeiriou, "Arcface: Additive angular margin loss for deep face recognition," in *CVPR*, 2019.
- [19] Le Hui, Xiang Li, Chen Gong, Meng Fang, Joey Tianyi Zhou, and Jian Yang, "Inter-Class Angular Loss for Convolutional Neural Networks," in *AAAI*, 2019.
- [20] Xiaoxu Li, Dongliang Chang, Tao Tian, and Jie Cao, "Large-margin regularized softmax cross-entropy loss," *IEEE Access*, vol. 7, pp. 19572–19578, 2019.

- [21] Dongliang Chang, Yifeng Ding, Jiyang Xie, Ayan Kumar Bhunia, Xiaoxu Li, Zhanyu Ma, Ming Wu, Jun Guo, and Yi-Zhe Song, “The devil is in the channels: Mutual-channel loss for fine-grained image classification,” *IEEE Transactions on Image Processing*, vol. 29, pp. 4683–4695, 2020.
- [22] Xinran Wei, Dongliang Chang, Jiyang Xie, Yixiao Zheng, Chen Gong, Chuang Zhang, and Zhanyu Ma, “FICAL: Focal Inter-Class Angular Loss for Image Classification,” in *VCIP*, 2019.
- [23] Tsung-Yi Lin, Priya Goyal, Ross Girshick, Kaiming He, and Piotr Dollár, “Focal loss for dense object detection,” in *ICCV*, 2017.
- [24] Jie Hu, Li Shen, and Gang Sun, “Squeeze-and-Excitation networks,” in *CVPR*, 2018.
- [25] Li Deng, “The MNIST database of handwritten digit images for machine learning research [best of the web],” *IEEE Signal Processing Magazine*, vol. 29, no. 6, pp. 141–142, 2012.
- [26] Alex Krizhevsky, Vinod Nair, and Geoffrey Hinton, “CIFAR-10 and CIFAR-100 datasets,” *URL: <https://www.cs.toronto.edu/kriz/cifar.html>*, vol. 6, 2009.
- [27] Jonathan Krause, Michael Stark, Jia Deng, and Li Fei-Fei, “3D Object Representations for Fine-Grained Categorization,” in *3DRR-13*, 2013.
- [28] Léon Bottou, “Large-scale machine learning with stochastic gradient descent,” in *COMPSTAT*. 2010.
- [29] Gao Huang, Yixuan Li, Geoff Pleiss, Zhuang Liu, John E Hopcroft, and Kilian Q Weinberger, “Snapshot ensembles: Train 1, get m for free,” *arXiv preprint arXiv:1704.00109*, 2017.
- [30] Kaiming He, Xiangyu Zhang, Shaoqing Ren, and Jian Sun, “Delving deep into rectifiers: Surpassing human-level performance on ImageNet classification,” in *ICCV*, 2015.
- [31] Harry O Posten, “The robustness of the one-sample t-test over the Pearson system,” *Journal of Statistical Computation and Simulation*, vol. 9, no. 2, pp. 133–149, 1979.